Two-Channel Kondo Physics in Two-Impurity Kondo Models

Andrew K. Mitchell,[1] Eran Sela,[1] and David E. Logan[2]

[1]*Institute for Theoretical Physics, University of Cologne, 50937 Cologne, Germany*
[2]*Department of Chemistry, Physical and Theoretical Chemistry, Oxford University,*
South Parks Road, Oxford OX1 3QZ, United Kingdom

We consider the non-Fermi-liquid quantum critical state of the spin-S two-impurity Kondo model and its potential realization in a quantum dot device. Using conformal field theory and the numerical renormalization group, we show the critical point to be identical to that of the two-channel Kondo model with additional potential scattering, for any spin S. Distinct conductance signatures are shown to arise as a function of device asymmetry, with the square-root behavior commonly believed to arise at low-energies dominant only in certain regimes.

Systems comprising several quantum impurities inherently display an interplay between impurity-bath and interimpurity couplings [1–7]: the tendency for impurities to be Kondo screened by conduction electrons competes with screening by interimpurity spin-singlet formation. Rich physics can thereby arise, as demonstrated, for example, in coupled quantum dots [7,8], magnetic impurities in metals [1], and recent two-impurity STM experiments [9]. Indeed, the same essential physics governs the analogous propensities for heavy fermion behavior or magnetic ordering in lattice systems [10].

The two-impurity, spin-$\frac{1}{2}$ Kondo model (2IKM) is the simplest to capture this competition [1]: local singlet formation is favored by an interimpurity exchange K, while coupling of each impurity to its own conduction channel favors separate Kondo screening below an effective single-channel, single-impurity scale T_K [2–5]. The lack of interchannel charge transfer in the 2IKM permits two distinct phases, and a quantum phase transition (QPT) results on tuning $K_c \sim T_K$. At the critical point, non-Fermi-liquid (NFL) physics arises below T_c, characterized [3] by anomalous properties such as fractional residual entropy and singular magnetic susceptibility.

This critical physics is also surprisingly robust to some perturbations, notably breaking of mirror (parity) symmetry or particle-hole symmetry [6]. Such perturbations are marginally irrelevant in the sense that the interimpurity coupling can be retuned to recover the critical point in all cases. But despite considerable effort, 2IKM critical physics has proved experimentally elusive—mainly due to interchannel charge transfer which smooths the QPT into a crossover [4]. Regular Fermi liquid (FL) physics then sets in below an energy scale T^*, and if the degree of charge transfer is large enough that $T^* \gg T_c$, no evidence of the critical point will be observed [11]. This is the situation relevant to the recent two-impurity experiments of Ref. [9]: coupling between one impurity on a metal surface and one

on a STM tip was also accompanied by strong tip-surface tunneling.

Reducing the degree of interchannel charge transfer might be possible in a quantum dot device such as that proposed in Ref. [6]. Provided $T^* \ll T_c$, NFL behavior should be observable in an intermediate energy window, as can be understood from a 2IKM critical perspective (indeed the eventual crossover to FL physics is wholly characteristic of the intermediate NFL state [12]).

An alternative route could, however, involve use of a quantum box, which acts as an interacting lead [13]. Coupling a single dot to one regular lead and one box tuned to the Coulomb blockade regime suppresses interchannel charge transfer completely. This has been exploited to access single-impurity two-channel Kondo (2CK) physics [14,15] in a real device [13]. Here we propose simply to interject a second dot in series between the "leads" to realize 2IKM physics. While parity and particle-hole symmetries are thereby broken, the QPT itself is unaffected. Robust NFL behavior should persist down to the lowest energy scales at the critical point.

Here we address two key questions in regard to potential realization of 2IKM physics. First, what is the nature of the critical point itself? We show that it is *identical* to that arising in a 2CK model with additional potential scattering, *independent* of parity breaking. Further, we show that the same QPT and 2CK critical point arises in the spin-S generalization of the 2IKM. Second, what are the signatures of criticality in measurable quantities such as conductance? These reflect renormalization group (RG) flow from higher-energy fixed points (FPs) and depend sensitively on parity breaking. We find, in particular, that the square-root behavior commonly anticipated [6,7] at low energies is absent in the standard channel-symmetric 2IKM.

Nature of 2IKM critical point.—The 2IKM reads:

$$H_{2\text{IKM}} = H_0 + H_{\text{ps}} + J_L \vec{S}_L \cdot \vec{s}_{0L} + J_R \vec{S}_R \cdot \vec{s}_{0R} + K \vec{S}_L \cdot \vec{S}_R,$$
(1)

where $H_0 = \sum_{\alpha,k} \epsilon_k \psi^\dagger_{k\sigma\alpha} \psi_{k\sigma\alpha}$ describes two free conduction channels $\alpha = L/R$, with density of states ρ, and spin density at the impurities $\vec{s}_{0\alpha} = \sum_{\sigma\sigma'} \psi^\dagger_{0\sigma\alpha} (\frac{1}{2}\vec{\sigma}_{\sigma\sigma'}) \psi_{0\sigma'\alpha}$ (where $\psi^\dagger_{0\sigma\alpha} = \sum_k \psi^\dagger_{k\sigma\alpha}$). Potential scattering is included via $H_{ps} = \sum_\alpha V_\alpha \psi^\dagger_{0\sigma\alpha} \psi_{0\sigma\alpha}$, and $\vec{S}_\alpha$ are spin-$\frac{1}{2}$ operators for the impurities. The 2IKM has been extensively studied using a number of powerful techniques [2–5,12], and certain similarities have been found [4–6,11,12] between it and the 2CK model [14,15],

$$H_{2\mathrm{CK}} = H_0 + H_{ps} + J_L \vec{S} \cdot \vec{s}_{0L} + J_R \vec{S} \cdot \vec{s}_{0R}, \qquad (2)$$

with $\vec{S}$ a spin-$\frac{1}{2}$ operator for a single impurity, exchange coupled to two independent conduction channels. The physics of the 2CK model is itself immensely rich [15]: the impurity is fully Kondo screened by the more strongly coupled conduction channel below an effective single-channel scale T_K, producing two distinct phases as a function of $(J_L - J_R)$. But when $J_L = J_R$, the frustration inherent when two channels compete to screen the impurity results in "overscreening," and NFL physics results below $T_K^{2\mathrm{CK}}$ [15]. Strikingly, both 2CK and 2IKM have the same fractional residual entropy, $S_{\mathrm{imp}} = \frac{1}{2}\ln(2)$.

Conformal field theory (CFT) has been used to describe the critical points of both models [4,16]. In the "unfolded" representation, H_0 is written in terms of left-moving chiral Dirac fermions. The CFTs for each model can be separated into different symmetry sectors. In particular, the $SU(2)_2 \times SU(2)_2 \times U(1)$ flavor, spin, and charge symmetries of the 2CK model [16] and the $U(1) \times U(1) \times SU(2)_2 \times Z_2$ left or right charge, total spin, and Ising symmetries of the 2IKM [3] can be exploited. The 2CK and 2IKM critical fixed point Hamiltonians take the same form as H_0, but with modified boundary conditions that affect only the spin sector of the 2CK model [16] or the Ising sector of the 2IKM [4]. The finite size spectrum (FSS) at the critical point of each model can then be determined [4,16]. In the channel-symmetric case $J_L = J_R$ and for $H_{ps} = 0$, the FSS of the 2CK critical point is characterized by the fractions $0, 1/8, 1/2, 5/8, 1, \ldots$, while for 2IKM a different FSS arises: $0, 3/8, 1/2, 7/8, 1, \ldots$

Despite these apparent differences between the critical FPs of the two models, the 2IKM can be mapped onto an effective 2CK model in special cases [5,6,11]. The key requirement for that mapping is of course the generation of an effective spin-$\frac{1}{2}$ local moment (LM), which can then be overscreened by symmetric coupling to two conduction channels. In the channel-asymmetric limit $J_L \gg J_R$, 2CK critical physics arises via a simple mechanism [6], first involving Kondo screening of the L impurity by the L lead on the single-channel scale T_K^L, followed by second-stage overscreening of the R impurity by the R lead and an effective coupling to the remaining Fermi liquid bath states of the L lead below T_c. An effective 2CK model of form Eq. (2), valid at low energies $T \lesssim T_K^L$, can be derived

formally using the approach of Ref. [17], exploiting the Wilson chain representation [18], and effective couplings follow as $\rho J_L^{\mathrm{eff}} \sim K/T_K^L$ and $\rho J_R^{\mathrm{eff}} \sim [1/\rho J_R - 1/\rho J_L]^{-1}$. The 2CK FP is thus stable when $K = K_c \sim T_K^L \rho J_R^{\mathrm{eff}}$, so the low-energy physics of the 2IKM is in this case wholly equivalent to that of the 2CK model.

Importantly, however, the L channel free electrons in the effective 2CK model acquire a $\pi/2$ phase shift due to the first-stage single-channel Kondo screening of the L impurity in the original 2IKM. This is seen clearly in the dynamics of the asymmetric 2IKM. To demonstrate this, and to highlight the basic physical picture, Fig. 1 shows spectra $D\rho_\alpha(\omega) \equiv -\pi\rho\,\mathrm{Im}[t_\alpha(\omega)]$ vs $|\omega|/D$ with $t_\alpha(\omega)$ the scattering t matrix [19]. Results are obtained from numerical renormalization group (NRG), exploiting all model symmetries, discretizing conduction bands of width $2D$ logarithmically using $\Lambda = 3$, and retaining 8000 states per iteration in each of $z = 3$ interleaved calculations (for a review, see Ref. [18]).

Single-channel Kondo screening of the L impurity by the L lead on the scale of T_K^L is seen directly in the L spectra in the upper panel of Fig. 1: a Kondo resonance, reaching the unitarity limit $D\rho_L = 1$, which has precisely the form of a regular single-channel Kondo (1CK) model [10]. This embodies the $\pi/2$ phase shift in the L channel, but no such feature is observed on this energy scale in the R spectra (lower panel of Fig. 1), indicating that the R impurity is still essentially free. On tuning the interimpurity coupling K closer to the critical point of the 2IKM,
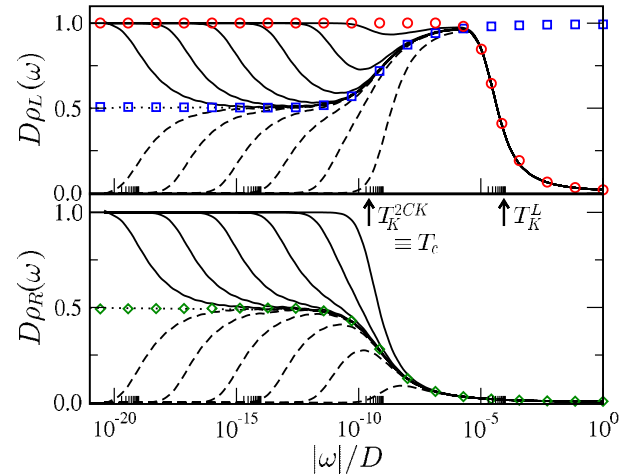

FIG. 1 (color online). Spectra $D\rho_\alpha(\omega)$ versus frequency $|\omega|/D$ for channels $\alpha = L$ and R (upper and lower panels, respectively) for the asymmetric 2IKM with fixed Kondo exchanges $\rho J_L = 0.1$, $\rho J_R = 0.05$, varying interimpurity exchange K (and $H_{ps} = 0$). Plotted using $K = K_c(1 \pm 10^{-n})$ for dashed lines and solid lines, with integer $n = 1 \rightarrow 6$ approaching progressively the critical point $K_c \sim T_K^L \approx 10^{-6}D$ (dotted line). Circles: A 1CK model with $\rho J = \rho J_L$. Diamonds: $D\rho_{2\mathrm{CK}}(\omega)$ for a pure 2CK model with $T_K^{2\mathrm{CK}} = T_c$. Squares: $D\tilde{\rho}_{2\mathrm{CK}}(\omega) = 1 - D\rho_{2\mathrm{CK}}(\omega)$.

the spectra in both channels fold progressively onto the critical spectra. For energies $|\omega|/D \ll T_K^L$, the critical spectrum $D\rho_R(\omega)$ is precisely that of a 2CK model $D\rho_{2CK}(\omega)$ with $T_K^{2CK} = T_c$. But the critical spectrum in the left channel is $D\rho_L(\omega) = 1 - D\rho_{2CK}(\omega)$ [17]. Thus, at the channel-asymmetric critical point [6],

$$D\rho_\alpha(\omega) \overset{|\omega| \ll T_c}{\sim} \tfrac{1}{2} + \alpha\beta\sqrt{|\omega|/T_c}, \qquad (3)$$

with $\alpha = \pm 1$ for channel L/R resulting from the additional L channel $\pi/2$ phase shift, and β a constant $\mathcal{O}(1)$.

This phase shift can be included in the 2CK model, Eq. (2), via the potential scattering term H_{ps} (i.e., $V_L \to \infty$ but $V_R = 0$, accompanied also by retuning J_L and J_R to access the critical point). This is equivalent to adding infinite uniform and staggered potential scatterings, which affect, respectively, the charge and flavor sectors of the 2CK model. Modifying the CFT for the critical point of the 2CK model to include this, we find [20] the boundary condition becomes equivalent to that of the 2IKM. The FSS is also naturally affected and is given by [20]

$$E_{2CK} = \tfrac{1}{8}(Q - a)^2 + \tfrac{1}{4}j(j + 1) + \tfrac{1}{4}j_F(j_F + 1) - bj_F^z, \quad (4)$$

where Q, j, and j_F are the charge, spin, and flavor quantum numbers. Uniform potential scattering shifts the charge parabolas, while staggered potential scattering biases the flavor sector. The $\pi/2$ phase shift in the L channel corresponds to $a = 1$ and $b = \tfrac{1}{2}$ [20]. Only certain quantum number combinations are allowed at the critical point, as given by the nontrivial gluing conditions derived in Ref. [16], and which reproduce fully the 2IKM spectrum when used with Eq. (4) (see Fig. 2 of [20]). One remarkable result obtained from our NRG calculations [20] is that the FSS at the critical point of the 2IKM does not depend on channel asymmetry (whence, in particular, the critical point possesses an emergent parity symmetry, irrespective of bare model symmetries). Further, we have shown [20] that the critical point for one model with potential scattering V_L and V_R is equivalent to the critical point of the other model with different potential scattering $\tilde{V}_L$ and $\tilde{V}_R$. The 2IKM and 2CK critical FPs are thus equivalent in the sense that they lie on the same marginal NFL manifold parametrized by H_{ps}.

Conductance line shapes and symmetry.—Full RG flow from the LM FP to the 2CK FP is thus recovered at the critical point of the asymmetric 2IKM. This is manifest [6] in the conductance arising, e.g., when a given channel $\alpha = L/R$ is split into source and drain. At zero bias, it is given exactly [21] in terms of the scattering t matrix (considered for the channel-asymmetric case in Fig. 1) by $G_{2IK}^\alpha(V_{sd} = 0, T)/(2e^2h^{-1}G_0^\alpha) = -\int_{-\infty}^\infty d\omega \, \partial f(\omega/T)/\partial\omega D\rho_\alpha(\omega, T)$, with $f(\omega/T)$ the Fermi function, and the impurity-lead coupling parametrized by $G_0^\alpha = 4\Gamma_s^\alpha\Gamma_d^\alpha/(\Gamma_s^\alpha + \Gamma_d^\alpha)^2$, in terms of the $\alpha = L/R$ hybridizations to source (Γ_s^α) and drain (Γ_d^α). Indeed, in

the limit $\Gamma_s^\alpha \gg \Gamma_d^\alpha$ (i.e., $G_0^\alpha \ll 1$), the $T = 0$ conductance follows as $\tilde{G}_{2IK}^\alpha(V_{sd}) = G_{2IK}^\alpha(V_{sd}, T = 0)/(2e^2h^{-1}G_0^\alpha) = D\rho_\alpha(\omega = V_{sd}, T = 0)$, and hence from Eq. (3) one finds at low energies $V_{sd} \ll T_c$,

$$\tilde{G}_{2IK}^\alpha(V_{sd}) = \tfrac{1}{2} + \alpha\beta\sqrt{V_{sd}/T_c} + \gamma_\alpha(V_{sd}/T_c) + \cdots, \quad (5)$$

where we include also a term linear in V_{sd}/T_c.

The leading square-root behavior of Eq. (5) has been viewed as the "smoking gun" signature of this 2CK physics [6,22], and was used to identify the critical point in the 2CK experiment of Ref. [13]. But we note that, unlike the 2CK model, the 2IKM does not possess $SU(2)$ flavor symmetry. Since symmetry dictates which operators can act in the vicinity of the critical FP, this is naturally reflected in the asymptotic conductance through the coefficients β and γ_α. Indeed, the full energy dependence of conductance depends on the unstable FPs, whose vying effects on RG flow again depend on symmetry and model parameters. For example, in the usual symmetric 2IKM [Eq. (1) with $J_L = J_R$ and $H_{ps} = 0$], no incipient LM is formed: there is no intermediate energy window with, e.g., $S_{imp} = \ln(2)$ entropy, and RG flow proceeds directly to the 2CK FP from the LM × LM high energy FP describing a pair of free impurities [$S_{imp} = \ln(4)$].

The effect of parity breaking is explored in Fig. 2, showing NRG results for conductance versus bias V_{sd} at the 2IKM critical point (obtained for $G_0^\alpha \ll 1$, as above). Conductance in the asymmetric limit $J_L \gg J_R$ is
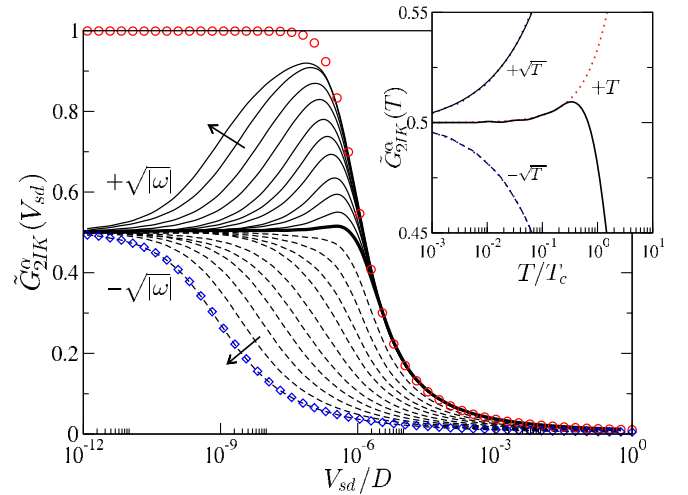

FIG. 2 (color online). $T = 0$ conductance $G_{2IK}^\alpha/(2e^2h^{-1}G_0^\alpha)$ through channel $\alpha = L$ and R (solid and dashed lines) versus bias V_{sd}/D, at the critical point. Shown for $\rho J_L = 0.075 \geq \rho J_R$, varying $\rho J_R = 0.075 \to 0.05$ in steps of 0.0025, with $K = K_c \sim T_{KL}^{1CK}$ retuned in each case (and $H_{ps} = 0$). Thick solid line is the symmetric case $J_L = J_R$; asymmetry $J_L/J_R \geq 1$ increases in direction of arrows. Circle and diamonds: Pure 1CK and 2CK scaling spectra. Inset: Zero-bias conductance versus T/T_c for $J_L/J_R = 1$ and 2 (and $\alpha = L, R$), exhibiting, respectively, leading linear and square-root behavior (dotted lines).

consistent with Ref. [6], and physical expectation as above [see Eq. (5)]. Here, the asymptotic conductance is $\tilde{G}^R_{2IK}(V_{sd}) \simeq 1 - \tilde{G}^L_{2IK}(V_{sd}) \equiv \tilde{G}_{2CK}(V_{sd})$ at low energies $V_{sd} \ll T^L_K$, where $T^L_K \gg T_c \equiv T^{2CK}_K$ and with $\tilde{G}_{2CK}(V_{sd})$ the conductance of the standard 2CK model [13,22] (diamonds). Thus, on exchanging $J_R \leftrightarrow J_L$, the coefficient β of Eq. (5) must change sign. But what happens as the asymmetry is decreased? We find the leading square-root contribution in Eq. (5) vanishes (see Fig. 2), as $\beta \sim (J_L - J_R)$, and leading *linear* behavior emerges at the symmetric point $J_L = J_R$ (the same naturally arising as a function of T at zero bias, see Fig. 2 inset). In fact, linear-V_{sd} behavior also emerges as the symmetric point is approached, since the square-root term dominates over a shrinking window $V_{sd}/T_c \ll (\beta/\gamma_\alpha)^2$.

Another striking feature of the conductance in more channel-symmetric situations is the behavior at higher T or energies $\gtrsim T_c \approx T^L_K$. Here the behavior is wholly characteristic of single-impurity, single-channel Kondo physics, as seen by comparison to the circles in Fig. 2.

The absence of square-root behavior in conductance of the symmetric 2IKM is contrary to common belief [6,7], so we now sketch our CFT proof [20]. As pointed out in Refs. [4,6], corrections to the t matrix in the vicinity of the critical point (whose ω dependence displays the same scaling as conductance) are determined from irrelevant boundary operators consistent with symmetry. Two such operators play a role here: $\delta H_1 = c_1 \epsilon'$ and $\delta H_2 = c_2 \vec{J}_{-1} \cdot \vec{\phi}$ (in the notation of Ref. [4]). The operator $\vec{J}_{-1} \cdot \vec{\phi}$ is the leading irrelevant operator of the 2CK FP, whose effect on the t matrix is known [23] to yield the famous square-root behavior. However, $\vec{J}_{-1} \cdot \vec{\phi}$ has *odd* parity in the 2IKM (unlike 2CK), which implies that its coefficient $c_2 \sim (J_L - J_R)$ vanishes in the symmetric limit. In both models, δH_1 does still contribute (c_1 always being finite [4]). One might naively expect ϵ' to behave similarly to $\vec{J}_{-1} \cdot \vec{\phi}$ since they have the same scaling dimension 3/2. However, the key difference between ϵ' and $\vec{J}_{-1} \cdot \vec{\phi}$ is that only the latter is a Virasoro primary field. Consequently [20], the leading square-root correction to the t matrix from δH_1 vanishes. In the symmetric 2IKM, the leading square-root behavior of conductance thus also vanishes.

Spin-S 2IKM.—Multilevel quantum dots can behave like $S = 1$ impurities [24], and high-spin impurities such as Co ($S = 3/2$) have been manipulated with STM [25]. Thus a natural and pertinent generalization of the 2IKM involves spin-S impurities: the model remains Eq. (1), but $\vec{S}_R$, $\vec{S}_L$ are now spin-S operators.

A QPT must again arise, as follows from the same line of argument as the spin-$\frac{1}{2}$ 2IKM [3]. On tuning K there is a phase-shift discontinuity on going from the local singlet phase for large K to a separated spin-S *underscreened* Kondo phase for small K. The nature of the transition arising at K_c is again clear by considering the asymmetric
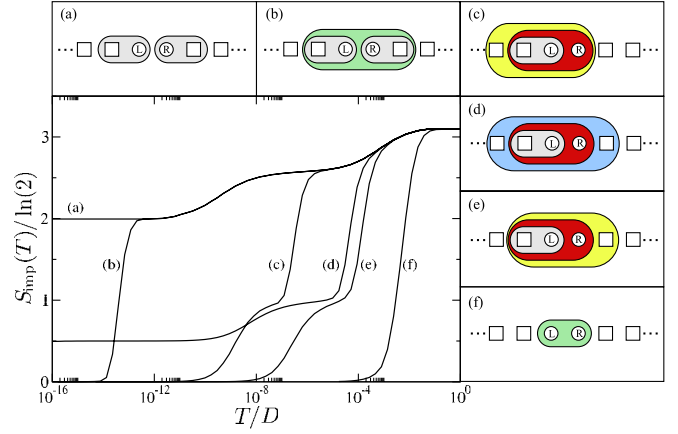

FIG. 3 (color online). Impurity entropy $S_{\text{imp}}(T)$ versus T/D for the 2IKM with spin-1 impurities. Plotted for fixed $\rho J_L = 0.15$, $\rho J_R = 0.05$, varying $K/D = 0, 10^{-13}, 3 \times 10^{-7}$, $K_c \approx 6 \times 10^{-5}, 2 \times 10^{-4}$, and 10^{-2} for lines (a)–(f). The corresponding physical processes are illustrated in panels (a)–(f): impurities denoted as circles and conduction band orbitals (in the Wilson chain representation [18]) as squares. For discussion, see text.

limit $J_L \gg J_R$. For concreteness consider $S = 1$, although the argument extends easily to higher S. NRG results for the entropy $S_{\text{imp}}(T)$ versus T are shown in Fig. 3, together with illustrations highlighting the key physical processes. In 3(a) the impurities are completely decoupled ($K = 0$), with each thus underscreened to a spin-$\frac{1}{2}$ by its attached lead α, on its own single-channel Kondo scale T^α_K [with residual entropy $2\ln(2)$]. For small finite $K < T^R_K$, 3(b), these residual moments form a local singlet state on the scale $T \sim K$, so the residual entropy is quenched. On increasing the interimpurity K further ($T^R_K < K < T^L_K$), the underscreened spin-$\frac{1}{2}$ L impurity and the still unscreened spin-1 R impurity are coupled and form a local doublet state on the scale $T \sim K$. This can then be single-channel Kondo screened by an effective coupling either to the L channel, 3(c), or the R channel, 3(e), and the residual entropy is again quenched. However, L and R effective couplings can become equal on fine-tuning K. This is the single spin-$\frac{1}{2}$ 2CK critical point, 3(d), with residual entropy $\frac{1}{2}\ln(2)$. For large $K \gg T^L_K$, a local interimpurity singlet state arises as expected, 3(f).

Analysis of the finite size spectrum at the critical point shows it to be *identical* to that of the regular spin-$\frac{1}{2}$ 2IKM, independent of asymmetry [20], and is hence that of a 2CK model with additional potential scattering.

Conclusion.—We have shown the critical point of the spin-S 2IKM, including the spin-$\frac{1}{2}$ variant, to be ubiquitously 2CK in nature. However, conductance line shapes measurable in experiment exhibit distinctive behavior depending on underlying symmetries, the low-energy behavior, in particular, evolving from square-root to linear behavior in V_{sd} or T as the channel-symmetric point is approached, and for any spin S.

[1] C. Jayaprakash, H. R. Krishna-murthy, and J. W. Wilkins, Phys. Rev. Lett. **47**, 737 (1981).

[2] B. A. Jones and C. M. Varma, Phys. Rev. Lett. **58**, 843 (1987).

[3] I. Affleck and A. W. W. Ludwig, Phys. Rev. Lett. **68**, 1046 (1992).

[4] I. Affleck, A. W. W. Ludwig, and B. A. Jones, Phys. Rev. B **52**, 9528 (1995).

[5] J. Gan, Phys. Rev. Lett. **74**, 2583 (1995).

[6] G. Zaránd, C.-H. Chung, P. Simon, and M. Vojta, Phys. Rev. Lett. **97**, 166802 (2006).

[7] A. M. Chang and J. C. Chen, Rep. Prog. Phys. **72**, 096501 (2009).

[8] W. G. van der Wiel *et al.*, Rev. Mod. Phys. **75**, 1 (2002).

[9] J. Bork *et al.*, Nature Phys. **7**, 901 (2011).

[10] A. C. Hewson, *The Kondo Problem to Heavy Fermions* (Cambridge University Press, Cambridge, England, 1993).

[11] F. W. Jayatilaka, M. R. Galpin, and D. E. Logan, Phys. Rev. B **84**, 115111 (2011).

[12] E. Sela, A. K. Mitchell, and L. Fritz, Phys. Rev. Lett. **106**, 147202 (2011).

[13] R. M. Potok, I. G. H. Shtrikman, Y. Oreg, and D. Goldhaber-Gordon, Nature (London) **446**, 167 (2007).

[14] P. Nozières and A. Blandin, J. Phys. (Paris) **41**, 193 (1980).

[15] D. L. Cox and A. Zawadowski, Adv. Phys. **47**, 599 (1998).

[16] I. Affleck and A. W. W. Ludwig, Nucl. Phys. **B360**, 641 (1991).

[17] A. K. Mitchell, D. E. Logan, and H. R. Krishnamurthy, Phys. Rev. B **84**, 035119 (2011).

[18] R. Bulla, T. Costi, and T. Pruschke, Rev. Mod. Phys. **80**, 395 (2008).

[19] A. K. Mitchell and D. E. Logan, Phys. Rev. B **81**, 075126 (2010).

[20] See Supplemental Material at http://link.aps.org/supplemental/10.1103/PhysRevLett.108.086405 for detailed derivation of the connection between the critical finite size spectra of 2CK and 2IKM, CFT analysis of the *t* matrix for the symmetric 2IKM, and further supporting numerical renormalization group calculations.

[21] Y. Meir and N. S. Wingreen, Phys. Rev. Lett. **68**, 2512 (1992).

[22] M. Pustilnik, L. Borda, L. I. Glazman, and J. von Delft, Phys. Rev. B **69**, 115316 (2004).

[23] I. Affleck and A. W. W. Ludwig, Phys. Rev. B **48**, 7297 (1993).

[24] D. E. Logan, C. J. Wright, and M. R. Galpin, Phys. Rev. B **80**, 125117 (2009).

[25] A. F. Otte *et al.*, Nature Phys. **4**, 847 (2008).

Two-channel Kondo physics in two-impurity Kondo models: Supplementary Material

Andrew K. Mitchell,[1] Eran Sela,[1] and David E. Logan[2]

[1]*Institute for Theoretical Physics, University of Cologne, 50937 Cologne, Germany*
[2]*Department of Chemistry, Physical and Theoretical Chemistry,*
Oxford University, South Parks Road, Oxford OX1 3QZ, United Kingdom

The following appendices comprise the supplementary material to Ref. 1.

I. CONNECTING THE FINITE SIZE SPECTRA OF THE TWO-CHANNEL AND TWO-IMPURITY KONDO MODELS

In this appendix we demonstrate that the critical points of the two-channel Kondo (2CK) model and the two-impurity Kondo model (2IKM) are connected by a marginal operator corresponding to the potential scattering H_{ps}. Specifically, the finite size spectrum of one model is shown to transform into that of the other model when this additional term is accounted for explicitly. In the channel-asymmetric 2IKM, the physical origin of this operator is readily understood from the mapping[2] between 2IKM and 2CK, where an additional phase shift in the more strongly-coupled channel arises due to first-stage single-channel Kondo screening of one of the impurities.

First, we review how the finite size spectrum at the critical point of the 2CK model is organized according to the unperturbed conformal field theory (CFT) with $U(1) \times SU(2)_2 \times SU(2)_2$ charge, spin and flavor symmetry sectors. The spectrum consists of Kac-Moody conformal towers, obtained by combining these symmetry sectors according to the gluing conditions[3] shown in Table I. The energy of the lowest lying state in each conformal tower (measured in units of $\frac{2\pi\hbar v_F}{L}$, with $v_F \equiv 1$ the Fermi velocity and $\hbar \equiv 1$ hereafter) follows from the formula[3]

$$E_{2CK} = \frac{Q^2}{8} + \frac{j(j+1)}{4} + \frac{j_F(j_F+1)}{4}, \tag{1}$$

where Q is the total charge, $j = 0, \frac{1}{2}, 1$ is the total spin, and $j_F = 0, \frac{1}{2}, 1$ is the flavor quantum number. Only certain quantum number combinations are allowed at the 2CK critical point,[3] as given by the nontrivial gluing conditions of Table I (and with level degeneracies also following from the Table). Also note that the gluing conditions for integer Q are defined modulo 2. Each conformal tower has an infinite number of states. Consider for example the spin j tower of the spin $SU(2)_2$ sector. The states with lowest energy form a spin j representation of $SU(2)$, and hence are $(2j+1)$-degenerate (the corresponding magnetic quantum number is $j_z = -j, -j+1, ..., j$). The reducible representations of $SU(2)$ with increasing spin (equal to j modulo 1) give rise to higher energy states. In the space of j_z and energy n, the envelope of an $SU(2)_k$ conformal tower on level k with spin j is $n = [(j^z)^2 - j^2]/k^4$. For a visualization of such unperturbed conformal towers, see the upper panels of Fig. 1.

We now perturb the CFT by introducing potential scattering $H_{ps} = \sum_\alpha V_\alpha \psi_{0\sigma\alpha}^\dagger \psi_{0\sigma\alpha}$. To see how this perturbation enters in the CFT, we first switch off the Kondo interactions, and consider free fermions of a single species $\sigma\alpha$. With antiperiodic boundary conditions $\psi_{\sigma\alpha}(-L/2) = -\psi_{\sigma\alpha}(L/2)$, the single particle momenta are $k = \frac{2\pi}{L}(n + \frac{1}{2})$; and for linear dispersion, the single particle energies are just given by k. The potential scattering amplitudes V_α can be parametrized in terms of scattering phase shifts δ_α. They are defined in terms of the shift of these single particle levels $k = \frac{2\pi}{L}(n + \frac{1}{2} - \frac{\delta_{\sigma\alpha}}{\pi})$. For $N_{\sigma\alpha}$ particles of each species, the correction to the total energy (again in units of $\frac{2\pi}{L}$)

Q	j	j_F	multiplicity	E_{2CK}
0	1/2	0	2	3/16
± 1	0	1/2	4	5/16
± 1	1	1/2	12	13/16
± 2	1/2	0	4	11/16
0	1/2	1	6	11/16

TABLE I: Nontrivial gluing conditions of conformal towers belonging to the $U(1) \times SU(2)_2 \times SU(2)_2$ charge, spin and flavor symmetry sectors.
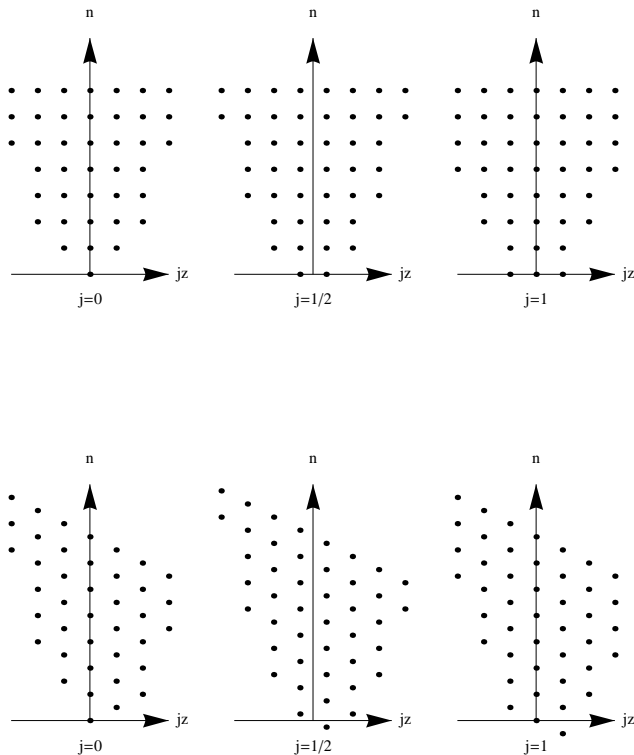
FIG. 1: Top panels: $SU(2)_k$ Kac-Moody conformal towers for $k = 2$, for $j = 0, \frac{1}{2}, 1$ from left to right. Bottom panels: tilted towers due to Zeeman term $-bj_F^z$ with $b = \frac{1}{2}$. Multiplicities are not shown.

is thus

$$\Delta E = -\frac{1}{\pi} \sum_{\sigma\alpha} \delta_{\sigma\alpha} N_{\sigma\alpha}. \tag{2}$$

In terms of the particle numbers, the total charge is $Q = \sum_\sigma (N_{\sigma L} + N_{\sigma R})$ while the magnetic quantum number of the flavor sector is $j_F^z = \frac{1}{2} \sum_\sigma (N_{\sigma L} - N_{\sigma R})$. In the presence of H_{ps}, the spectrum thus follows as $\tilde{E}_{2CK} = E_{2CK} + \Delta E$, viz

$$\tilde{E}_{2CK} = \frac{Q^2}{8} + \frac{j(j+1)}{4} + \frac{j_F(j_F+1)}{4} - Q\frac{\delta_L + \delta_R}{2\pi} - j_F^z \frac{\delta_L - \delta_R}{\pi}, \tag{3}$$

where $\delta_{\sigma\alpha} \equiv \delta_\alpha$ since the potential scattering H_{ps} is independent of spin σ. Eq. (3) is equivalent to Eq. (4) of Ref. 1, with $a = 2\frac{\delta_L + \delta_R}{\pi}$ and $b = \frac{\delta_L - \delta_R}{\pi}$. Thus H_{ps} simply biases the charge and flavor conformal towers. For a visualization of the effect on the $SU(2)_2$ flavor towers, see the lower panels of Fig. 1. The spectrum obtained using the trivial free fermion gluing conditions[3] describes free electrons but with the additional potential scattering. Importantly, switching on H_{ps} and switching on the Kondo interactions commute, since there is a spin-charge-flavor separation in the model.[3] Employing instead the nontrivial gluing conditions of Table I in Eq. (3), we thus obtain the 2CK critical spectrum including the influence of H_{ps}.

In Fig. 2, we examine the evolution of the energy levels at the critical point of the 2CK model as function of δ_L for $\delta_R = 0$, plotting the lowest excitation energies $\delta E_i = \tilde{E}_i - \min\{\tilde{E}_i\}$. The fractions $0, \frac{1}{8}, \frac{1}{2}, \frac{5}{8}, 1...$ correspond to multiplets of the symmetry $U(1) \times SU(2)_2 \times SU(2)_2$ of the regular 2CK model. Those multiplets split due to the flavor field and charge field induced by finite H_{ps}, but eventually at $\delta_L = \pi/2$ they recombine to give new multiplets characterized by the fractions $0, \frac{3}{8}, \frac{1}{2}, \frac{7}{8}, 1...$, and which correspond to that of the regular 2IKM.[5]

To strengthen the connection between the two models, we now consider the effect of H_{ps} on the critical CFT of the 2IKM itself. We exploit here the Bose-Ising representation[5] of the 2IKM, consisting of a decomposition into $SU(2)_1 \times SU(2)_1 \times SU(2)_2 \times Z_2$ left/right charge (isospin), total spin and Z_2 Ising symmetry sectors. The z-component of $\alpha = L$ or R isospin is essentially the total charge of channel α. Specifically, its magnetic quantum number is given
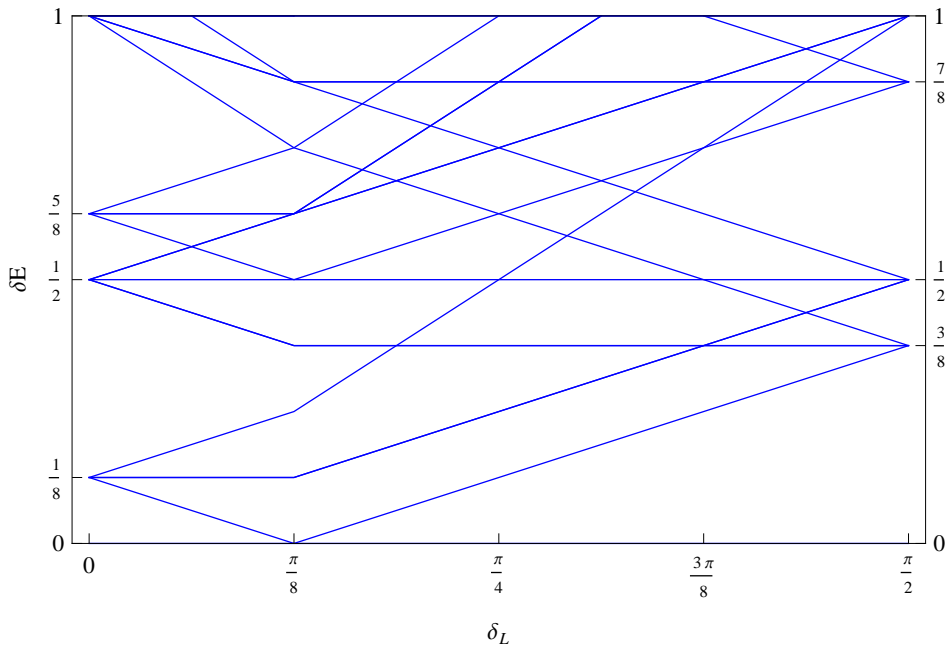
FIG. 2: Excitation energies δE according to Eq. (3) as a function of δ_L for $\delta_R = 0$, connecting the regular 2CK spectrum ($\delta_L = 0$) and the 2IKM spectrum ($\delta_L = \pi/2$). Note that at $\delta_L = \pi/8$ the ground state changes from the doublet $(Q, j, j_F) = (0, 1/2, 0)$ to the $j_F^z = 1/2$, $Q = 1$ component of the quintet $(\pm 1, 0, 1/2)$.

simply by $i_\alpha^z = \frac{1}{2} \sum_\sigma N_{\sigma\alpha}$ in terms of the particle numbers. Using Eq. (2), it follows that $\Delta E = -\frac{2}{\pi} \sum_\alpha \delta_\alpha i_\alpha^z$. The energy of the lowest states of each conformal tower in the 2IKM with the additional potential scattering term H_{ps} is thus $\tilde{E}_{2IK} = E_{2IK} + \Delta E$, where E_{2IK} is given in Ref. 5. Our final result is

$$\tilde{E}_{2IK} = \frac{i_L(i_L + 2)}{3} + \frac{i_R(i_R + 2)}{3} + \frac{j(j+1)}{4} + x_{\text{Ising}} - 2\frac{\delta_L}{\pi}i_L^z - 2\frac{\delta_R}{\pi}i_R^z, \tag{4}$$

where, $i_\alpha = 0, \frac{1}{2}$ are the isospin quantum numbers, $j = 0, \frac{1}{2}, 1$ is the total spin quantum number and $x_{Ising} = 0, \frac{1}{16}, \frac{1}{2}$ (corresponding to the unity operator, spin field σ, and fermion field ϵ of the Z_2 Ising model). The nontrivial gluing condition of the $SU(2)_1 \times SU(2)_1 \times SU(2)_2 \times Z_2$ sectors is given in Table. III of Ref. 5, and gives the finite size spectrum of the 2IKM in the presence of potential scattering.

Using Eqs. (3) and (4) with their corresponding gluing conditions, we find

$$\mathcal{H}_{CP}^{2IK}(\delta_L, \delta_R) = \mathcal{H}_{CP}^{2CK}(\delta_L + \pi/2, \delta_R), \tag{5}$$

where $\mathcal{H}_{CP} \equiv \{\delta E_i\}$ at the critical point of either model, parametrized in terms of the free fermion phase shifts δ_L and δ_R. The finite size spectrum at the critical point of one model with potential scatterings V_L and V_R is identical to that of the other model with different $\tilde{V}_L$ and $\tilde{V}_R$ when the phase shifts satisfy Eq. (5). Thus, the critical fixed points (FPs) are equivalent in the sense that they lie on the same marginal manifold parametrized by H_{ps}.

A. Alternative formulation in terms of Majorana fermions

Having drawn the connection between the non-abelian CFT formulation of the 2CK and 2IKM, we discuss now the same relation within the framework of abelian bosonization.

The steps applied first by Emery and Kivelson[6] as an alternative solution to the 2CK model, and later by Gan[7] in the 2IKM context, are as follows. (i) Bosonize separately each chiral fermionic species (with the impurities at the 'boundary' located at $x = 0$), $\psi_{\sigma\alpha}(x) \sim e^{-i\phi_{\sigma\alpha}(x)}$. (ii) Define linear combinations of the bosonic fields $\phi_{\sigma\alpha}(x)$, $\{\phi_c, \phi_s, \phi_f, \phi_X\} = \frac{1}{2}\sum_{\sigma,\alpha=1}^2 \phi_{\sigma\alpha}\{1, (-1)^{\sigma+1}, (-1)^{\alpha+1}, (-1)^{\sigma+\alpha}\}$, corresponding to charge, spin, flavor and spin-flavor bosons ($A = c, s, f, X$). (iii) Define four new fermionic species by $\psi_A(x) \sim e^{-i\phi_A(x)}$, whose real ($\chi_1^A = \frac{\psi_A^\dagger + \psi_A}{\sqrt{2}}$) and

imaginary ($\chi_2^A = \frac{\psi_A^\dagger - \psi_A}{\sqrt{2}i}$) parts give eight Majorana fermions (MFs) $\chi_j^A(x)$, (with $j = 1, 2$ and $A = c, s, f, X$), which may be regarded as components of the vector $\vec{\chi}(x)$. The Hamiltonian for the free theory with $J_L = J_R = 0$ and $H_{ps} = 0$ is then $H = \frac{i}{2} \int_{-\infty}^{\infty} dx \, \vec{\chi}(x) \cdot \partial_x \vec{\chi}(x)$, with the trivial boundary condition (BC) $\vec{\chi}(0^+) = \vec{\chi}(0^-)$. The BC relates the field before scattering at $x = 0^+$ and after scattering at $x = 0^-$ (using a left moving convention). The remarkable fact is that in both 2CK and 2IKM, the critical FP Hamiltonian is the same as that of the free theory, but with a modified BC that is also simple in terms of the MFs. For 2CK it is simply[3]

$$\vec{\chi}_s(0^+) = -\vec{\chi}_s(0^-) \qquad \text{and} \qquad \chi_j^A(0^+) = \chi_j^A(0^-) \ \text{ for } \ (A, j) \neq (s, 1), (s, 2), (X, 1), \tag{6}$$

with $\vec{\chi}_s = (\chi_1^s, \chi_2^s, \chi_1^X)$, such that the modified BC affects only the spin sector of the 2CK model. For 2IKM,[8]

$$\chi_2^X(0^+) = -\chi_2^X(0^-) \qquad \text{and} \qquad \chi_j^A(0^+) = \chi_j^A(0^-) \ \text{ for } \ (A, j) \neq (X, 2), \tag{7}$$

where the modified BC here affects only the Ising sector of the 2IKM.

An *odd* number of MFs suffer the modified BC in both models. This is a hallmark of non-Fermi liquid (NFL) behavior, as it implies[8] a vanishing amplitude for scattering of an electron into an electron. By contrast, the BCs for Fermi liquids always involve an even number of MFs, corresponding thereby to linear BCs for regular fermions.

Besides their common NFL character, the different BCs for the critical points of the 2CK and 2IKM do not immediately suggest any connection between the models. However, we now show that adding potential scattering in one channel of the 2CK model (Eq. (2) of Ref. 1, with $V_L \to \infty$ and $V_R \to 0$ in the added term H_{ps}) causes a change in the critical 2CK BC which makes it equivalent to that of the 2IKM.

As above, the addition of infinite potential scattering in the left channel (which results in the desired $\delta_L = \pi/2$ phase shift) is equivalent to the addition of infinite uniform potential scattering $\frac{1}{2}\psi_L^\dagger \psi_L + \frac{1}{2}\psi_R^\dagger \psi_R = i\chi_2^c \chi_1^c$ which affects only the charge sector, and infinite staggered potential scattering $\frac{1}{2}\psi_L^\dagger \psi_L - \frac{1}{2}\psi_R^\dagger \psi_R = i\chi_2^f \chi_1^f$, affecting only the flavor sector. Since both charge and flavor sectors are unaffected by the Kondo interaction (which acts purely in the *spin* sector), the resulting behavior can be understood from the response of free fermions to potential scattering in the simpler situation $J_L = J_R = 0$. For $V_L \to \infty$ and $V_R \to 0$, modified BCs are conferred to the charge and flavor MFs: $\chi_{1,2}^{c,f}(0^+) = -\chi_{1,2}^{c,f}(0^-)$. Together with the BC from Eq. 6, we now obtain the BC for the critical 2CK model in the presence of the potential scattering, viz

$$\chi_2^X(0^+) = \chi_2^X(0^-) \qquad \text{and} \qquad \chi_j^A(0^+) = -\chi_j^A(0^-) \ \text{ for } \ (A, j) \neq (X, 2). \tag{8}$$

This BC is the same as that of the 2IKM, Eq. (7), except for an additional minus sign afflicting the BC for all MFs. However, the BCs corresponding to Eqs. (7) and (8) are in fact equivalent in the 2CK model, as now shown.

An 'overall' minus sign in the BC for the MFs can be interpreted as a phase shift felt by each of the charge, spin, flavor and spin-flavor fermions, defined in terms of the scattering process $\psi_A(0^-) = \exp(2i\delta_A)\psi_A(0^+)$, and with $\delta_A = \pi/2$ for $A = c, s, f, X$. Since the number operators for ψ_A fermions are related[9] to the number operators for the regular $\psi_{\sigma\alpha}$ fermions via $\{N_c, N_s, N_f, N_X\} = \frac{1}{2}\sum_{\sigma\alpha} N_{\sigma\alpha}\{1, (-1)^{\sigma+1}, (-1)^{\alpha+1}, (-1)^{\sigma+\alpha}\}$, it follows that $\sum_A N_A = 2N_{\uparrow L}$. In terms of the particle numbers N_A, the correction to the total energy due to additional phase shifts is $\Delta E = -\frac{1}{\pi}\sum_A \delta_A N_A = -N_{\uparrow L}$. Comparing to Eq. 2, we then find that $\delta_{\uparrow L} = \pi$ (and $\delta_{\sigma\alpha} = 0$ for $\sigma\alpha \neq \uparrow L$). Thus the additional global minus sign in the BCs for the MFs equates to $\psi_{\uparrow L}(0^-) = \exp(2i\delta_{\uparrow L})\psi_{\uparrow L}(0^+) \equiv \psi_{\uparrow L}(0^+)$ for the original fermions, and so has no effect on the finite size spectrum — or on the lowest-energy physics in general.

II.   CORRECTION TO THE GREEN FUNCTION NEAR THE 2IKM CRITICAL POINT

In this appendix we consider corrections to the critical FP Hamiltonian of the 2IKM, and from them construct corrections to the Green function. We show that the nature of these corrections (which show up in physical quantities such as conductance) is characteristic of the NFL behavior, and depend distinctively on parity breaking in the model.

A.   Fixed point Hamiltonian of the 2IKM

First we construct the list of operators allowed by symmetry in the generic asymmetric 2IKM (see Eq. (1) of Ref. 1), including the dependence on small $J_L - J_R$ and on small potential scattering amplitudes V_L and V_R. We rely on the same operator content obtained by Affleck and Ludwig,[5] based on the $SU(2)_1 \times SU(2)_1 \times SU(2)_2 \times Z_2$ symmetry decomposition. The critical FP of the symmetric 2IKM without potential scattering has only one irrelevant operator of dimension $3/2$, denoted ϵ', and is given by Eq. (5.1) of Ref. 5. In the present context where parity and particle-hole

i_L	i_R	j	Ising	x
0	0	0	1	0
$\frac{1}{2}$	0	$\frac{1}{2}$	σ	$\frac{1}{2}$
0	$\frac{1}{2}$	$\frac{1}{2}$	σ	$\frac{1}{2}$
0	0	1	1	$\frac{1}{2}$
0	0	0	ϵ	$\frac{1}{2}$
$\frac{1}{2}$	$\frac{1}{2}$	0	1	$\frac{1}{2}$
0	0	1	ϵ	1
$\frac{1}{2}$	$\frac{1}{2}$	1	1	1
$\frac{1}{2}$	$\frac{1}{2}$	0	ϵ	1
$\frac{1}{2}$	$\frac{1}{2}$	1	ϵ	$\frac{3}{2}$

TABLE II: Operator content of the 2IKM critical FP.

symmetries are in general broken, additional operators are allowed, and in fact dominate the approach to the NFL FP.

Each operator that can occur at an unstable FP is either a primary operator or a descendant of it.[5] The primary operators are labeled with the same quantum numbers $(i_1, i_2, j, \text{Ising})$ used to label states in Eq. (4). The particular combinations of $SU(2)_1 \times SU(2)_1 \times SU(2)_2 \times Z_2$ left/right isospin, total spin and Ising operators, together with their scaling dimension x, was obtained using the double fusion method in Ref. 5. For clarity and completeness we reproduce that list here in Table II.

In general, the presence of a given symmetry implies that the only allowed operators are those which are singlets of that symmetry. In particular, the full $SU(2)_1 \times SU(2)_1 \times SU(2)_2 \times Z_2$ symmetry of the standard 2IKM with $H_{ps} = 0$ gives rise to the leading singlet operator $(i_1, i_2, j, \text{Ising}) = (0, 0, 0, \epsilon)$. This relevant operator is associated[5] with the perturbation $(K - K_c)$, which destabilizes the 2IKM critical point. At the critical point $K = K_c$, one leading irrelevant operator[5] is the descendant of $(0, 0, 0, \epsilon)$, denoted $\mathcal{O}_1 = \epsilon' \approx \partial_\tau \epsilon$. Since ϵ has scaling dimension $1/2$, its first descendant has scaling dimension $3/2$. But singlets can also be obtained as descendants of primary $SU(2)$ fields with integer spin. Indeed, the other singlet operator with dimension $3/2$ is in this case obtained by acting on the $\vec{\phi} = (0, 0, 1, 1)$ primary vector field of the $j = 1$ spin sector with an operator that creates spin excitations.[5] Thus, one must consider also a second irrelevant operator $\mathcal{O}_2 = \vec{J}_{-1} \cdot \vec{\phi}$ (where $\vec{J}_{-1}$ is the lowest Fourier mode of the spin current creating such excitations).

Since $\vec{J}_{-1} \cdot \vec{\phi}$ is also the leading irrelevant operator in the 2CK model,[10] one might expect the physical behavior stemming from it to be common to both 2CK and 2IKM. However, the crucial difference between the models is that $\vec{J}_{-1} \cdot \vec{\phi}$ has odd parity in the 2IKM but even parity in the 2CK model; as now shown.

Parity symmetry (corresponding to left/right reflection in space) is defined by invariance under the permutations $\vec{S}_L \leftrightarrow \vec{S}_R$ and $\psi_L \leftrightarrow \psi_R$. One rather subtle consequence[5] of parity symmetry in the 2IKM is that $\vec{\phi} \to -\vec{\phi}$. This can be seen from the parity-odd operator $\psi_L^\dagger \vec{\sigma} \psi_L - \psi_R^\dagger \vec{\sigma} \psi_R = \vec{\phi} \epsilon$ (and noting that ϵ is the operator corresponding to $(K - K_c)$, and is as such unaffected by the reflection, $\epsilon \leftrightarrow \epsilon$). Thus $\vec{J}_{-1} \cdot \vec{\phi}$ is also parity-odd in the 2IKM. But in the 2CK model, $\psi_L^\dagger \vec{\sigma} \psi_L - \psi_R^\dagger \vec{\sigma} \psi_R = \vec{\phi} \phi_F^z$. Here, $\vec{\phi}_F$ is the $j_F = 1$ primary field of the flavor sector, and ϕ_F^z is its z-component. Since parity corresponds to a π rotation around the x flavor direction in the 2CK model, the flavor current $\vec{J}_F = \sum_\sigma \psi_\sigma^\dagger \frac{\vec{\tau}}{2} \psi_\sigma$ transforms as $J_F^x \to J_F^x$, $J_F^{y,z} \to -J_F^{y,z}$; and similarly $\phi_F^x \to \phi_F^x$, $\phi_F^{y,z} \to -\phi_F^{y,z}$. Thus $\vec{J}_{-1} \cdot \vec{\phi}$ is parity even in the 2CK model. Of course, this is the expected result here since $\vec{J}_{-1}$ and $\vec{\phi}$ are both spin operators, but the parity transformation affects only the flavor sector of the 2CK model.

Finally, we consider the additional operators appearing when isospin $SU(2)_1 \times SU(2)_1$ symmetry is broken (but spin $SU(2)$ symmetry is maintained), as occurs when potential scattering from H_{ps} is included. Specifically, $H_{ps} = 2 \sum_\alpha V_\alpha I_\alpha^z(x = 0)$, where the z-component of the channel-α isospin current is given by $I_\alpha^z(x) = \frac{1}{2} \sum_\sigma \psi_{\sigma\alpha}^\dagger(x) \psi_{\sigma\alpha}(x)$. Since V_α does not couple to fields with half-integer isospin, and the primary operators have total spin $j = 0$, then it follows that V_α couples only to dimension $3/2$ descendants of the $(0, 0, 0, \epsilon)$ field. Thus, two further dimension $3/2$ operators $\mathcal{O}_{3,4} = (I_{L,R}^z)_{-1} \epsilon$ are obtained (where $(\vec{I}_\alpha)_{-1}$ is the isospin analogue of the spin operator $\vec{J}_{-1}$ discussed above). No other dimension $3/2$ operators are consistent with the symmetry.

The corrections to the critical FP Hamiltonian in the presence of H_{ps} thus comprise four operators,

$$\delta H = \frac{1}{\sqrt{T_c}} \sum_{i=1}^{4} c_i \mathcal{O}_i. \tag{9}$$

As shown in Ref. 5, the coefficient $c_1 \sim 1$. By contrast, the odd transformation property of $\mathcal{O}_2$ under parity implies

$$c_2 \sim \left(\frac{J_L - J_R}{J_L + J_R} \right) \tag{10}$$

for small small $(J_L - J_R)$. Finally $c_{3,4} \propto V_{L,R}$ for small $V_{L,R}$.

In the conformal limit (which relies upon linear dispersion and infinite conduction bandwidth), the Bose-Ising representation of the 2IKM reads $H_{2IK} = H_0 + \vec{J}(0) \cdot (J_L \vec{S}_L + J_R \vec{S}_R) + \vec{\phi}(0)\epsilon \cdot (J_L \vec{S}_L - J_R \vec{S}_R) + 2 \sum_\alpha V_\alpha I_\alpha^z(0)$, showing that there is perfect separation of isospin and Ising sectors (although there is a coupling between Ising and spin via the term $\vec{\phi}(0)\epsilon$). Since $\mathcal{O}_{3,4}$ involve coupling between isospin and Ising operators $(I_{L,R}^z)_{-1}$ and ϵ, in this idealized limit one thus obtains $c_{3,4} = 0$ identically. But in generic models, one naturally expects $c_{3,4} \ll 1$ to be finite but small. For this reason we ignore the operators $\mathcal{O}_{3,4}$ in the present work.

However, we do note that the $\mathcal{O}_{3,4}$ operators do play a significant role in variants of the standard 2IKM which contain explicit coupling between isospin and Ising or spin sectors. The two-impurity Anderson model is a pertinent example: the low-energy effective model[5,11] is a 2IKM but with additional terms such as $\psi^\dagger (\vec{\sigma} \tau^x) \psi \cdot (\vec{S}_L + \vec{S}_R)$. These terms mix the spin and isospin sectors, leading thereby to indirect coupling between $(I_{L,R}^z)_{-1}$ and ϵ operators, and hence in such situations $c_{3,4}$ are not expected to be small.

B. Corrections to the Green function

Corrections to the t matrix and conductance in the vicinity of the 2IKM critical point are directly related to corrections to the single particle Green function.[10] Ignoring the operators $\mathcal{O}_{3,4}$ as above, the leading correction to the Green function to first order in Eq. (9) is $\delta G(z_1, z_2) = \delta_1 G(z_1, z_2) + \delta_2 G(z_1, z_2)$, where

$$\delta_1 G(z_1, z_2) = \frac{c_1}{\sqrt{T_c}} \int_0^\beta d\tau \langle \psi(z_1) \epsilon'(0, \tau) \psi^\dagger(z_2) \rangle,$$

$$\delta_2 G(z_1, z_2) = \frac{c_2}{\sqrt{T_c}} \int_0^\beta d\tau \langle \psi(z_1) \vec{J}_{-1} \cdot \vec{\phi}(0, \tau) \psi^\dagger(z_2) \rangle, \tag{11}$$

and $\beta = 1/T$ is inverse temperature. Here we suppress the spin and channel indices, and use $z_1 = \tau_1 + ir_1$, $\bar{z}_2 = \tau_2 + ir_2$. Assuming $r_1 > 0$ and $r_2 < 0$, the propagator is sensitive to scattering from the impurities at the boundary located at $r = 0$. The calculation of $\delta_2 G(z_1, z_2)$ was performed by Affleck and Ludwig,[10] who exploited the fact that the three-point function in $\delta_2 G(z_1, z_2)$ is fully determined by conformal invariance (up to an overall constant) since $\vec{J}_{-1} \cdot \vec{\phi}$ is a Virasoro primary. The electron and Ising fields, ψ and ϵ, are chiral fields with scaling dimension $1/2$, and thus[10]

$$\delta_2 G(z_1, z_2) \propto \frac{c_2}{\sqrt{T_c}} \left(\frac{\pi}{\beta} \right)^{5/2} \times$$

$$\int_0^\beta d\tau \frac{[\sin \frac{\pi}{\beta}(z_1 - z_2)]^{1/2}}{\left[\sin \left(\frac{\pi}{\beta}(\tau - z_1) \right) \sin \left(\frac{\pi}{\beta}(\tau - z_2) \right) \right]^{3/2}}. \tag{12}$$

The τ integral can be expressed in terms of hypergeometric functions, which yield asymptotically the famous $\sqrt{\omega}$ energy-dependence of the related t matrix.[10]

The integrand in $\delta_1 G(z_1, z_2)$ is similarly a three point function, but $\epsilon' \approx \partial_\tau \epsilon$ is not a Virasoro primary field. However, ϵ itself is Virasoro primary. Pulling the derivative out of the correlation function, one obtains

$$\delta_1 G(z_1, z_2) = \frac{c_1}{\sqrt{T_c}} \int_0^\beta d\tau \partial_\tau \langle \psi(z_1) \epsilon(0, \tau) \psi^\dagger(z_2) \rangle \propto$$

$$\frac{c_1}{\sqrt{T_c}} [\sin \frac{\pi}{\beta}(z_1 - z_2)]^{-1/2} \left(\frac{\pi}{\beta} \right)^{3/2} \int_0^\beta d\tau \partial_\tau \frac{1}{\left[\sin \left(\frac{\pi}{\beta}(\tau - z_1) \right) \sin \left(\frac{\pi}{\beta}(\tau - z_2) \right) \right]^{1/2}} = 0. \tag{13}$$
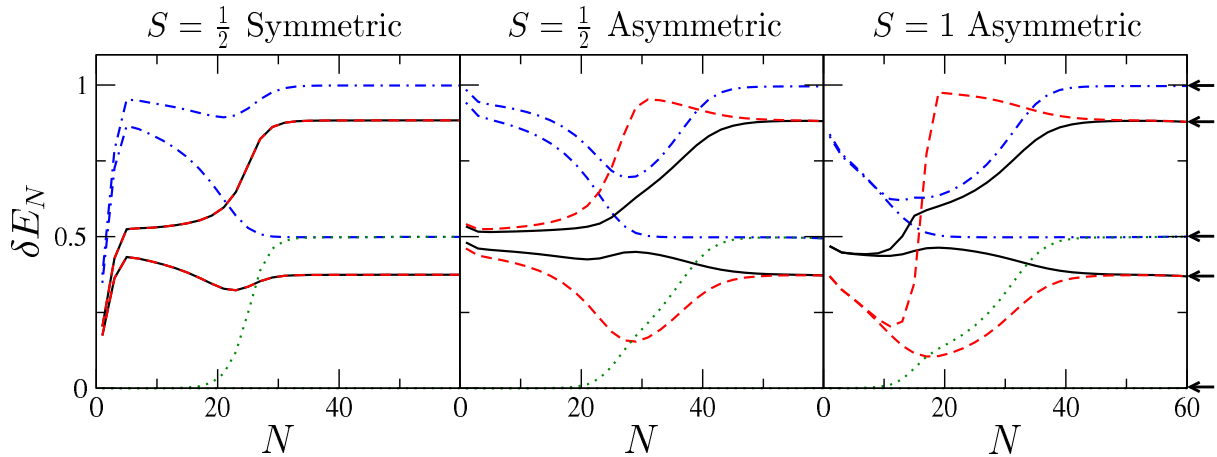
FIG. 3: NRG energy levels δE_N for odd iteration number, N. The lowest 2 levels are shown in each left/right charge and total spin subspace with quantum numbers $(Q_L, Q_R, S_{tot}^z) = (0, 0, 0)$ [dotted lines], $(0, 1, \frac{1}{2})$ [solid lines], $(1, 0, \frac{1}{2})$ [dashed lines] and $(1, 1, 0)$ [dot-dashed lines]. *Left panel*: symmetric spin-$\frac{1}{2}$ 2IKM with $\rho J_L = \rho J_R = 0.075$. *Middle panel*: asymmetric spin-$\frac{1}{2}$ 2IKM with $\rho J_L = 0.075$ and $\rho J_R = 0.05$. *Right panel*: asymmetric spin-1 2IKM with $\rho J_L = 0.15$ and $\rho J_R = 0.05$. Interimpurity coupling $K \simeq K_c$ tuned to its critical value in each case, and $H_{ps} = 0$.

The integrand has no singularities as long as z_1 and z_2 are away from the boundary, and no branch cuts associated with the square-root function are intersected. Periodicity in β then implies that the integral vanishes, and so the contribution to the Green function from $\delta_1 G(z_1, z_2)$ also vanishes. Thus, the anomalous square-root correction to the Green function must come from $\delta_2 G(z_1, z_2)$ alone. In particular, our conclusion is that the coefficient of the square-root energy-dependence of the t matrix and hence conductance is proportional to c_2, which vanishes in the symmetric 2IKM, obtained as $J_L \to J_R$.

Higher-order corrections to the Green function can be calculated in a similar fashion. In particular, the correction coming from the next order in perturbation theory involves integrals such as $\int_0^\beta d\tau \int_0^\beta d\tau' \langle \psi(z_1) \mathcal{O}_i(0, \tau) \mathcal{O}_i(0, \tau') \psi^\dagger(z_2) \rangle$. Since such integrals contains singularities when $\tau \to \tau'$, the correction does not in general vanish, even when ∂_τ and $\partial_{\tau'}$ are pulled outside the correlator in the case of $\mathcal{O}_1 = \epsilon'$. Such calculations are notoriously involved; and here necessitate the use of an ultraviolet cutoff $\mathcal{O}(T_c)$ to avoid unphysical divergences. The leading correction is however expected to yield a *linear* energy dependence (albeit up to possible log corrections), in agreement with our numerical renormalization group calculations, see Fig. 2 of Ref. 1.

III. 2IKM CRITICAL PHYSICS WITHIN THE NUMERICAL RENORMALIZATION GROUP

In this appendix we consider the role of parity breaking on the RG flow, finite size spectrum and thermodynamics of the 2IKM. Such information can be extracted from numerical renormalization group (NRG) calculations,[12] as now briefly reviewed.

Since its first application to the single-impurity single-channel Kondo model,[12] Wilson's NRG technique has been used successfully to study a wide range of quantum impurity problems (for a comprehensive recent review, see Ref. 13). More recently, the increase in computing resources has permitted the detailed analysis of two-channel models involving several impurities, such as the 2IKM considered in the present work.

The key element of the NRG technique[12,13] is a logarithmic discretization of the free conduction electron Hamiltonian, H_0. The continuum of states in each conduction band is divided into intervals with discretization points $x_n = \pm D \Lambda^{-n}$ (here $n = 0, 1, 2, ...$ and $2D$ is the bandwidth), and whose width thus decreases exponentially as the Fermi level is approached. A single state (the symmetric linear combination) is then retained in each interval, such that low-energies are exponentially-well resolved. Canonical transformation by tridiagonalization yields the Wilson chain representation,[12,13] where each conduction channel corresponds to a semi-infinite chain terminated by the impurity sub-system. The discretized Hamiltonian is then diagonalized iteratively: starting from the impurity, Wilson chain orbitals are coupled on successively and the system diagonalized. To avoid exponential growth of the Hilbert space, high-energy states are discarded after each step. This truncation scheme correctly allows calculation of the lowest-energy eigenenergies $\{E_N\}$ of a finite Wilson chain of length N because the coupling between the Wilson chain orbitals N and $(N + 1)$ scale as $\Lambda^{-N/2}$. In consequence,[12,13] high-lying states at one iteration do not cross over and
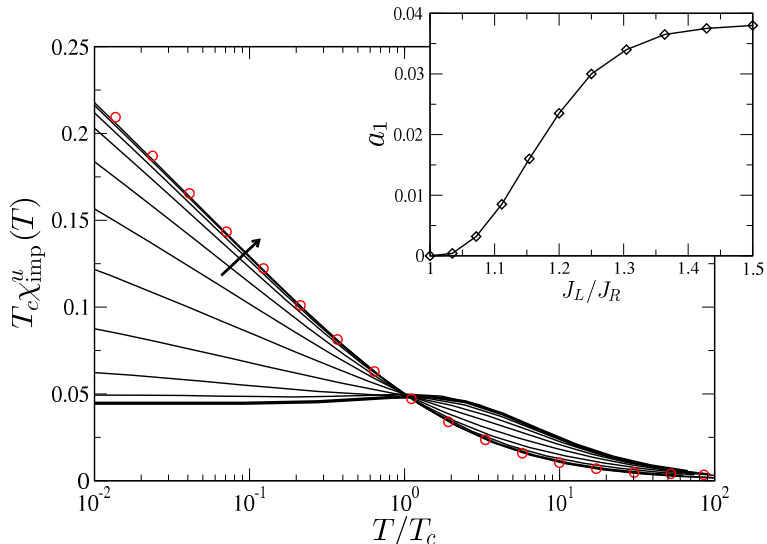
FIG. 4: Uniform magnetic susceptibility $T_c\chi_{\text{imp}}^u(T)$ vs temperature T/T_c for the 2IKM model. Shown for $\rho J_L = 0.075 \geq \rho J_R$, varying $\rho J_R = 0.075 \to 0.05$ in steps of 0.0025, with $K = K_c$ retuned in each case (and $H_{ps} = 0$), as in Fig. 2 of Ref. 1. Thick solid line is the symmetric case $J_L = J_R$; asymmetry $J_L/J_R \geq 1$ increases in direction of the arrow. Circle points for a 2CK model with $T_K^{2CK} \equiv T_c$. Inset shows the variation of the slope a_1 as a function of J_L/J_R (see Eq. 14). $a_2 \approx 0.05$ is essentially independent of asymmetry. We have defined T_c here through $T_c\chi_{\text{imp}}^u(T_c) = 0.05$.

become low-lying states at a later iteration due to the energy scale separation inherent when $\Lambda > 1$.

$\delta E_N(i) = \Lambda^{N/2}(E_N(i) - \min\{E_N\})$ are rescaled many-particle energies (indexed i and measured with respect to the ground state energy), and span roughly the same energy range, independent of N. The evolution of these levels with N can be understood in terms of an RG flow,[12,13] with the various fixed points giving characteristic spectra which do not change upon further iteration. Indeed, the lowest energy levels at the stable fixed point (obtained as $N \to \infty$) reproduce accurately the finite size spectrum obtained by CFT.[14]

Thermodynamics can also be calculated from these NRG energy levels.[12,13] The essential step here is the identification of a characteristic temperature $T_N \sim \Lambda^{-N/2}$, at which thermodynamic quantities can be accurately calculated for a given finite iteration N. This temperature is chosen to be high enough that the splitting of the levels incurred at later iterations does not affect the thermodynamic calculation; but not too high that states above the truncation limit contribute significantly. Thus useful physical information can be extracted from each iteration, and so the full temperature-dependence of thermodynamic quantities can be built up.

A. Effect of parity-braking on RG flow and finite size spectrum

In Fig. 3 we show the evolution of low-lying NRG eigenenergies δE_N with iteration number (Wilson chain length) N, for 2IKMs at criticality. Specifically, we compare the channel-symmetric and -asymmetric spin-$\frac{1}{2}$ 2IKM and the asymmetric spin-1 2IKM (with $H_{ps} = 0$ in each case). The RG flow, as evidenced by the flow of these levels, is manifestly different for the three cases considered. In particular, levels with left/right charge and total spin quantum numbers $(Q_L, Q_R, S_{\text{tot}}^z) = (0, 1, \frac{1}{2})$ and $(1, 0, \frac{1}{2})$ are of course degenerate in the symmetric 2IKM (left panel), since the Hamiltonian is invariant on swapping L and R labels. By contrast no such symmetry of the bare Hamiltonian is present in the channel-asymmetric spin-$\frac{1}{2}$ or spin-1 2IKMs plotted in the middle and right panels; and thus levels related by $L \leftrightarrow R$ permutation are not in general degenerate.

Importantly however, an emergent parity symmetry at the stable NFL fixed point is observed, with $(Q_L, Q_R, S_{\text{tot}}^z)$ and $(Q_R, Q_L, S_{\text{tot}}^z)$ levels becoming degenerate as $N \to \infty$.

Indeed, the set of NFL fixed point levels in each case is identical, demonstrating that the stable fixed point itself is identical, irrespective of bare model symmetries, and independent of spin-S. The fixed point levels are indicated by the arrows, and correspond to the fractions 0, $\frac{3}{8}$, $\frac{1}{2}$, $\frac{7}{8}$, 1, ..., as obtained for the regular symmetric 2IKM by CFT.[5]

B. Effect of parity-braking on thermodynamics

We turn now to thermodynamics, focusing on the 'impurity' contribution[12,13] to the uniform spin susceptibility, $\chi_{\text{imp}}^u(T) = \langle (\hat{S}_{\text{tot}}^z)^2 \rangle_{\text{imp}}/T$ (here $\hat{S}_{\text{tot}}^z$ refers to the spin of the entire system and $\langle \hat{\Omega} \rangle_{\text{imp}} = \langle \hat{\Omega} \rangle - \langle \hat{\Omega} \rangle_0$, with $\langle \hat{\Omega} \rangle_0$ denoting a thermal average in the absence of the impurities).

In the 2CK model, the uniform susceptibility diverges logarithmically[15,16] at low temperatures $T \ll T_K^{2CK}$,

$$T_K^{2CK} \chi_{\text{imp}}^u(T) = a_1 \ln(T_K^{2CK}/T) + a_2. \tag{14}$$

One naturally expects the uniform susceptibility of the 2IKM to behave similarly in the channel-asymmetric limit (with $T_K^{2CK} \equiv T_c$), since here there is a mapping to the 2CK model.[2] However, as pointed out in Ref. 5, the uniform susceptibility is *not* singular in the regular symmetric 2IKM. Rather, it is the staggered susceptibility that is divergent in this case.

In Fig. 4 we show how the uniform susceptibility $T_c \chi_{\text{imp}}^u(T)$ vs temperature T/T_c evolves with increasing asymmetry for the spin-$\frac{1}{2}$ 2IKM. In the case of large channel asymmetry ($J_L/J_R = 1.5$), the behavior is indeed that of Eq. (14), with coefficients a_1 and a_2 essentially those of the regular 2CK model (see comparison to the pure 2CK case, circle points). But, in analogy to the vanishing square-root energy dependence of conductance at the symmetric point, we find that the coefficient $a_1 \to 0$ as $J_L/J_R \to 1$ (see inset). Indeed, the leading contribution to the uniform susceptibility in this limit can be understood[3] from second-order perturbation theory in the leading irrelevant operator $\mathcal{O}_2 = \vec{J}_{-1} \cdot \vec{\phi}$. From Eq. (10) it then follows that $a_1 \propto (J_L - J_R)^2$ for small $(J_L - J_R)$. Thus, there is a smooth crossover between the limiting cases, with divergent 2CK behavior arising in the asymmetric limit, but constant uniform susceptibility as $T \to 0$ emerging at the symmetric point, consistent with Ref. 5.

---

[1] A. K. Mitchell, E. Sela and D. E. Logan, Phys. Rev. Lett. (2012)

[2] G. Zaránd, C.-H. Chung, P. Simon, and M. Vojta, Phys. Rev. Lett. **97**, 166802 (2006).

[3] I. Affleck and A. W. W. Ludwig, Nucl. Phys. B **360**, 641 (1990).

[4] I. Affleck, D. Gepner, H. J. Schulz and T. Ziman J. Phys. A: Math. Gen. **22** 511 (1989).

[5] I. Affleck, A. W. W. Ludwig, and B. A. Jones, Phys. Rev. B **52**, 9528 (1995).

[6] V. J. Emery and S. Kivelson, Phys. Rev. B **46**, 10812 (1992).

[7] J. Gan, Phys. Rev. Lett. **74**, 2583 (1995).

[8] J. M. Maldacena and A. W. W. Ludwig, Nucl. Phys. B **565**, 506 (1997).

[9] G. Zaránd and J. von Delft, Phys. Rev. B **61**, 6918 (2000).

[10] I. Affleck and A. W. W. Ludwig, Phys. Rev. B **48**, 7297 (1993).

[11] F. W. Jayatilaka, M. R. Galpin, and D. E. Logan, Phys. Rev. B **84**, 115111 (2011).

[12] K. G. Wilson, Rev. Mod. Phys. **47**, 773 (1975).

[13] R. Bulla, T. Costi, and T. Pruschke, Rev. Mod. Phys. **80**, 395 (2008).

[14] Strictly, the finite size spectrum is obtained on taking the $\Lambda \to 1$ limit.[17] However, the lowest fixed point levels of the NRG recover the CFT spectrum to within a few percent for $\Lambda = 3$, as employed in the present work.

[15] N. Andrei and C. Destri, Phys. Rev. Lett. **52**, 364 (1984).

[16] A. M. Tsvelik, J. Phys. C **18**, 159 (1985).

[17] R. Bulla, A. C. Hewson, and G.-M. Zhang, Phys. Rev. B **56**, 11721 (1997).